



**INSTITUTE FOR SUSTAINABLE ENERGY, UNIVERSITY OF MALTA**

***SUSTAINABLE ENERGY 2013:  
THE ISE ANNUAL CONFERENCE***

Thursday 21st March 2013, Dolmen Hotel, Qawra, Malta

**ASSESSING THE OFFSHORE WAVE ENERGY POTENTIAL FOR THE MALTESE ISLANDS**

Drago A.<sup>1</sup>, Azzopardi J.<sup>1</sup>, Gauci A.<sup>1</sup>, Tarasova R.<sup>1</sup>, Bruschi A.<sup>2</sup>

<sup>1</sup>Physical Oceanography Unit, IOI-Malta Operational Centre,  
University of Malta, Msida, MSD2080, Malta  
Tel: (+356) 21440972

<sup>2</sup>Istituto Superiore per la Protezione e la Ricerca Ambientale,  
Institute for Environmental Protection and Research,  
Via V. Brancati 60, 00144, Roma, Italy  
Tel: (+39) 06-50074589

Corresponding Author email: [aldo.drago@um.edu.mt](mailto:aldo.drago@um.edu.mt)

**ABSTRACT**

Direct wave observations using a Datawell buoy deployed to the west of Gozo, and a numerical wave modeling exercise targeted to map the spatial and temporal signatures of the wave fields around the Maltese Islands over a span of five years (1st January 2007 to 31st December 2011) have been conducted within the BLUE OCEAN ENERGY<sup>®</sup> project. This has provided a detailed characterization of local wave climates and an estimation of the available wave energy potentials in the coastal and offshore areas of the Maltese Islands. This data is essential to assess the overall feasibility of constructing wave energy production farms based on WECs, to test the most adequate devices to harvest wave energy, as well as to identify the best candidate sites for an optimal and most economically practical extraction. The study reveals that the best sites in the Maltese waters would be those located at the western approaches to the islands, given that these are more exposed to the prevailing North-Westerly winds. At these sites, maximum significant wave heights can exceed 7 m in winter, even in close proximity to the coast, and with a seasonal mean of 1.92 m as determined from direct measurements. The mean wave power transport during the winter season is estimated at 15 kW m<sup>-1</sup>; the wave resource is more than halved in spring and even weaker in autumn; it is under 2 kW m<sup>-1</sup> during summer. Stronger wave fields occur at a few kilometres to the South West of Filfla Island where the modelled mean wave power reaches values of 13 kW m<sup>-1</sup> in the winter months, but at less accessible sites and greater distances from shore.

Keywords: Wave Energy, Renewable Energy, Numerical Modelling, Marine Observations

## **1. INTRODUCTION**

### **1.1 Wave Energy Extraction**

Marine-based renewable energy technologies are set to be further developed and exploited for energy extraction from the sea. In Europe, such endeavours are set within the proclaimed target of the EU to raise the share of renewable energy supply to 20% by 2020. In the case of the Maltese Islands, the very restricted space available on land is compensated by the highest ratio (>12) amongst European nations of available marine space with respect to land territory,

considering the extent of territorial waters up to 12 nautical miles. Sea depths increase rapidly around most of the coast [1], especially on the southern perimeter of the Maltese Islands (refer to Figure 1), and this poses a constraint on the location of offshore wind energy extraction installations. On the other hand, energy production from sea waves constitutes a likely avenue for supporting energy demands through the use of renewables, especially in environments where deeper waters are in closer proximity to grid connections at the coast, and wave climates are not excessively wild to hamper the mooring and functioning of wave energy converters

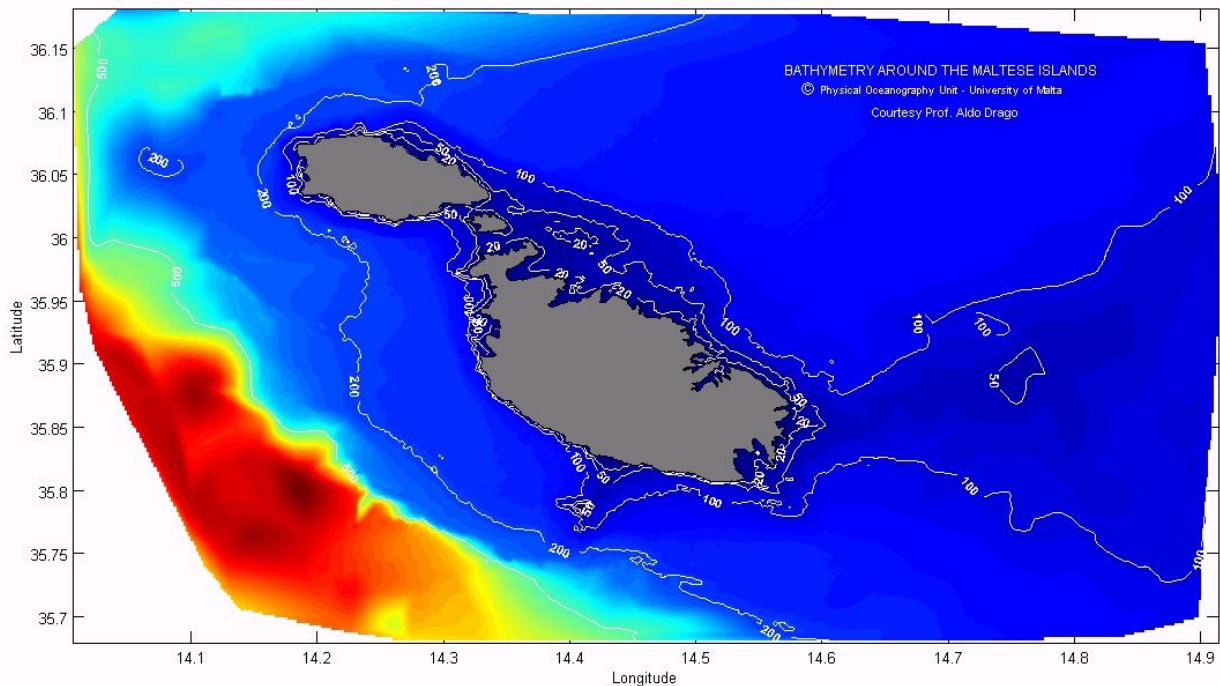


**Figure 1:** Bathymetry around the Maltese Islands [1] © Physical Oceanography Unit, University of Malta

(WECs). The potential in Malta of extracting energy from sea waves is thus believed to be worth considering at least as an additional or complementary resource.

Wave power (in  $\text{kW m}^{-1}$ ) is expressed in terms of the energy flux carried by unit length of a wavefront. The wave energy resource in the Mediterranean Sea is about an order of magnitude lower than that observed at the ocean looking Western European coasts. In the band of latitudes between  $40\text{--}60^\circ\text{N}$ , offshore wave power levels can exceed  $60 \text{ kW m}^{-1}$ , equivalent to an average annual wave energy source of 120 GW [2]. In the relatively sheltered North Sea where the practice of wave energy extraction is most prolific, the available wave resource is considerably lower, but still feasible for extraction; values range from less than  $6 \text{ kW m}^{-1}$  ( $\approx 10\text{TWh}$  annually) in Sweden to maxima of the order of  $23\text{--}50 \text{ kW m}^{-1}$  ( $\approx 400\text{TWh}$  annually) near Norway [3]. The stretch of deep sea in the North-West Mediterranean is influenced by the channelling of Mistral winds resulting in a highly agitated wave climate in the area and an estimated maximum yearly mean wave power in the range of  $13\text{--}15 \text{ kW m}^{-1}$  [4]; long term wave observations made by a buoy of the Italian Wave Network on the western coast of Sardinia confirm annual wave power values of  $9.1 \text{ kW m}^{-1}$  averaged over more than 18 years of data [5]. Wave intensity is attenuated, but remains somewhat relevant in the

deep Ionian Sea; it diminishes further in the Levantine Basin; other locations in sheltered areas like the Adriatic Sea and near the rest of the Mediterranean coast offer very little wave power potential. By virtue of the central location of the Maltese Islands in the Sicily Channel, the wave climate is expected to offer a good potential; this is especially relevant in the case of WEC concepts that can combine (i) a high performance in exploiting the wave characteristics pertaining to relatively deeper water environments close to the shoreline with (ii) favourable mooring solutions and a reduced risk against structural damage in case of extreme harsh conditions.

## 1.2 Previous studies

A first attempt to study the wave climatology in the Sicilian Channel and the Maltese Islands was conducted by the Physical Oceanography Unit (PO-Unit) of the IOI-Malta Operational Centre at the University of Malta within the Interreg IIB MEDOCC WERMED (Weatherouting dans la Méditerranée) Project [6] [7]. In the absence of direct measurements, a numerical wave modeling approach was adopted using the high-resolution wave data base for the period 1958-2001 compiled from the EU R&D HIPOCAS project (*Hindcast of Dynamic Processes of the Ocean and Coastal Areas of Europe*). Hourly values of wave parameters were derived from a run of the WAM wave model [8]

over the Mediterranean with a grid resolution of  $0.5^\circ$ , and with two grids used in a 2-way nesting mode: one over the Eastern Mediterranean with  $0.25^\circ$  resolution and another over the Central Mediterranean with  $0.125^\circ$  resolution. Monthly time series of 44-year of hourly values of  $H_s$ ,  $Wdir$ ,  $T_m$  and  $T_p$  at every grid point in the area of interest were derived. Statistical analysis of these monthly time-series was done by calculation of maximum, minimum, mean values and standard deviation, as well as the 99<sup>th</sup>, 90<sup>th</sup>, 75<sup>th</sup>, 50<sup>th</sup> and 25<sup>th</sup> percentile for each parameter. The analysis provided a description of the spatial and temporal variability of wave intensity and incidence in the region, including information on extreme events.

With Seabased, (a Swedish company), on behalf of Vigourtech Ltd, the PO-Unit also supported an initial feasibility study to identify the potential of setting up wave farms in the vicinity of the Maltese Islands using arrays of point absorbers with a linear generator situated at the sea bottom and based on the OWEC wave energy counter rotating generator. Such systems mainly consist of underwater buoys that can be deployed with minimal visual impact, and without excessive limitations imposed by sea depth. A wave energy farm with 40,000 units would be expected to occupy an area of approximately  $20\text{Km}^2$  (0.52% of total marine space under Maltese jurisdiction) with an estimated installed capacity of 400 MW [9].

### 1.3 The Blue Ocean Energy project

This paper deals with the research done by the PO-Unit within the BLUE OCEAN ENERGY<sup>®</sup> project ([www.capemalta.net/blueoceanenergy/](http://www.capemalta.net/blueoceanenergy/)), led by DEXAWAVE Energy Malta Ltd and funded by the National Research & Innovation Programme (2010) of the Malta Council for Science & Technology. The main project deliverable is the testing of a prototype WEC, and the assessment on the feasibility of the use of this technology to furnish the Maltese Islands with clean energy. In the project the PO-Unit was responsible to observe and model the wave characteristics of the seas around the Maltese Islands, while the Institute of Sustainable Energy (ISE) endeavoured to analyse the WEC design and compatibility with the local wave characteristics.

The average annual available wave power is a critical factor in determining the economic worth for investing in sea wave energy exploitation at a site, but the seasonal variability and the intrinsic wave characteristics are also important factors. There is no single fitting WEC technology option that applies universally at all sites; WEC design needs to match the site specific spectral wave characteristics

to harvest maximal outputs from the range of signals that carry most of the energy.

In this specific assessment data on the wave potential around the Maltese Islands was recorded by means of a dedicated Datawell wave buoy deployed 2Km off the Northwest coast of Gozo, as well as by wave resource mapping using numerical modelling techniques. In this paper the computer-based models used in the assessment are first described. The in-situ wave measurements recorded by the buoy are then described and compared to the model data. The final part of the paper is dedicated to the wave resource mapping.

## 2. WAVE MODELS

The numerical wave modeling exercise is intended to map the spatial and temporal signatures of the wave fields around the Maltese islands. Two nested wave models, the Malta MARIA WAM model at coarser resolution ( $0.125^\circ$ ) and the higher resolution ( $0.002^\circ$ ) embedded Malta SWAN model, were set up and run over a span of five years (1st January 2007 to 31st December 2011); the time span is considered to be sufficient to identify the different wave conditions at seasonal, annual and inter-annual time scales.

### 2.1 Malta MARIA WAM model

The Malta MARIA WAM model uses the 3rd generation spectral wave model WAM Cycle 4 [10]. The basic equation used by the model is the wave action balance equation with a wave field spectrum in the two-dimensional frequency and direction space. The energy equation is forced by a source term related to the near-surface atmospheric wind. The model is forced by 6-hourly surface wind fields with  $0.5^\circ$  resolution derived from the Malta MARIA/Eta atmospheric forecasting system also run operationally by the PO-Unit [6]. The wave model is set-up as a 2-step nested system starting from a coarse grid covering the whole Mediterranean region at a resolution of  $0.50^\circ$  in both longitude and latitude direction. The intermediate grid domain is nested within the coarse grid and covers the Eastern Mediterranean region (east of  $10^\circ$  E) with grid resolution of  $0.25^\circ$ . A further high-resolution grid (resolution of  $0.125^\circ$ ) over the Central Mediterranean is nested within the intermediate East Mediterranean grid. The model is based on the following run-time parameters: 30 frequencies (in the range from 0.041772 to 0.66264 Hz); 24 directions (every 15 degree); 3 output grids; 4916 sea points; and 3-hour outputs. The time integration step is 1200 sec. The main output parameters from the WAM wave model are:

significant wave height; mean wave direction and frequency of total sea; wind sea and swell. Figure 2 shows the domain of the WAM model set up over the Central Mediterranean.

## 2.2 Malta SWAN model

The WAM model is not optimised to simulate coastal and near-coast conditions, and its spatial resolution does not permit the bathymetry and coastline to be detailed sufficiently. More refined wave conditions were thus derived by using the higher resolution SWAN model.

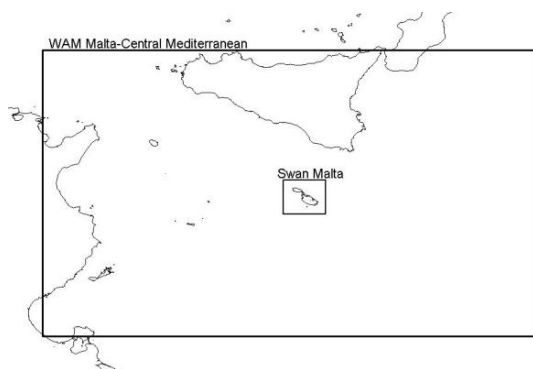


**Figure 2:** Domains of the Malta WAM Central Mediterranean and Malta SWAN models

SWAN is a third-generation wave model using the same formulations of WAM for the source terms and based on the wave action balance equation with sources and sinks [11]. It is typically applied on any scale relevant for wind-generated surface gravity waves to obtain realistic estimates of wave parameters in coastal areas, lakes and estuaries from given wind, sea bottom and current conditions. The SWAN model solves the spectral action balance equation without any a priori restrictions on the spectrum for the evolution of wave growth. This equation represents the effects of spatial propagation, refraction, shoaling, generation, dissipation and nonlinear wave-wave interactions. While the WAM model considers problems on oceanic scales, with SWAN the wave propagation is calculated from deep water up to the surf zone. Since WAM makes use of explicit propagation schemes in geographical and spectral spaces, it requires very small grid sizes in shallow water and is thus unsuitable for applications to coastal regions. On the other hand SWAN employs implicit schemes, which are more robust and economic in shallow water.

## 2.3 Model implementation

The near-coast wave conditions around the Maltese Islands were obtained by running SWAN in hindcast mode for 5 consecutive years (between

1st January 2007 and 31st December 2011) on a regular grid over the domain defined by 14.040-14.700° in longitude and 35.665-36.206° in latitude. The spatial resolution of 0.002° is defined by 331 and 271 grid cells in the x- and y-directions respectively. At its lateral boundaries SWAN is nested to the coarser scale WAM model into which it is embedded; boundary conditions are derived from wave spectral information of the best 24 hr Malta MARIA WAM model forecast fields. At the surface it is forced by wind data from the Malta MARIA ETA atmospheric forecasting model; sea currents are prepared from the hydro-dynamical shelf scale eddy-resolving ROSARIO-6420 forecasting model, ([www.capemalta.net/MFSTEP/results0.html](http://www.capemalta.net/MFSTEP/results0.html)). The SWAN model generates output fields every 3 hours of the following key parameters: Significant Wave Height; Peak Period of the variance density spectrum; Mean Absolute Wave Period; Mean Wave Direction.

## 3. IN SITU MEASUREMENTS

Long term *in situ* sea wave measurements by moored systems provide accurate information spanning different temporal and spatial scales, but data is representative only of a restricted localised area around the station position. Numerical models are thus used to extrapolate this information in space and in time, providing synoptic views over extensive spatial domains with projections in past (hindcasts) and future (forecasts) times. Nonetheless modelling on its own does not provide a complete solution since direct measurements are necessary to validate and fine tune numerical models; buoy data provide a means of assessing the performance of computer models by skill diagnostics based on comparisons between model and field observations.

A second major activity of the PO-Unit within the Blue Ocean Energy project consisted in the deployment in early fall of 2011 of a Datawell Waverider buoy (WR-SG) at about 2 Km offshore the north-western coast of Gozo in a depth of about 200m (refer to Figure 3). Such an instrument utilises a stabilized platform sensor to track the vertical component of the orbital wave motion, and is capable of measuring reliable wave height measurements with a resolution of up to 1cm [12]. Prior to deployment, the seabed and mooring procedure were carefully studied to ensure the successful operation of the buoy. The bottom part of the mooring consists of an anchor weight to keep the system from drifting while the first fifteen meters are made of rubber cord. The buoy is connected to the cord by a stabilizing chain.



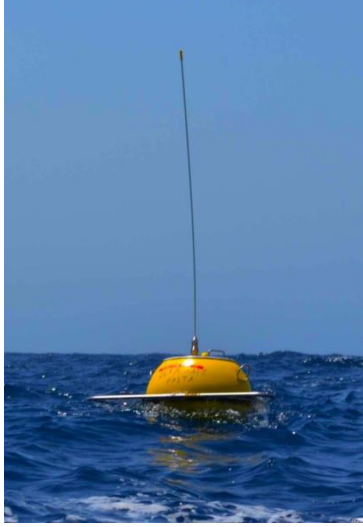


**Figure 3:** Datawell Waverider buoy deployed in a location west of the Gozo coastline

The hardware and microprocessor are powered by batteries inside the hull. Measurements consist of the Significant Wave Height  $H_s$  (mean crest-to-trough height in meters of the highest one third of the waves), the Zero Up-crossing Period  $T_z$  (average time between two successive point crossings of the mean sea level), the maximum power spectral density (in  $m^2/Hz$ ), and the battery voltage. Data is transmitted in real-time via UHF with a temporal frequency of about 1.1Hz. Every 30 minutes, the system also sends the GPS coordinates measured by an onboard receiver. The receiving radiometric equipment is installed at the Gharb Local Council in Gozo around 4.4km away from the anchor position, and is directly connected to the internet by means of the Ethernet port. Dedicated software prepared to decode and store the received signals runs in operational mode on one of the PO-Unit's servers at the University of Malta. To avoid any loss of data, the buoy also records the measured data on an onboard Compact Flash (CF) card. Recovery of the saved file requires the towing of the buoy and the hull to be opened. Real-time data is viewed through a web interface that was developed to deliver data as well as to keep track of the buoy's location. The GPS position is constantly monitored, and if a location outside a predefined zone is detected, a warning is issued via email and SMS to all partners of the project. This allows for early action in case of vandalism or an anchor drift.

Even though the buoy has one accelerometer and can only record wave height, the position and anchor information are used to estimate the applied strain direction. In particular, the distance between the two coordinates is computed by the Haversine equation to get the shortest distance over the Earth's surface between the two points. If the coordinates of the buoy are given by  $(lon_1, lat_1)$  and

the anchor position is  $(lon_2, lat_2)$ , then the distance can be found as follows:

$$\Delta lon = lon_2 - lon_1$$

$$\Delta lat = lat_2 - lat_1$$

$$a = \sin^2\left(\frac{\Delta lat}{2}\right) + \cos(lat_1)\cos(lat_2)\sin^2\left(\frac{\Delta lon}{2}\right)$$

$$c = 2 \times \text{atan2}(\sqrt{a}, \sqrt{1-a})$$

$$d = R \times c$$

where  $R$  is the earth's radius (6371km).

The bearing angle that gives the direction of the buoy from the anchor position is also found by the forward azimuth formula which gives a direction between  $-180^\circ$  and  $+180^\circ$ . This is defined as:

$$\theta = \text{atan2}[\sin(\Delta lon)\cos(lat_2), \cos(lat_1)\sin(lat_2) - \sin(lat_1)\cos(lat_2)\cos(\Delta lon)]$$

#### 4. WAVE POWER CALCULATIONS AT THE BUOY LOCATION

Not all sites in a marine domain are suitable for wave energy exploitation. The suitability of a location is usually determined on the basis of the average annual (or even monthly) available wave power, and the dominant mean wave direction. These physical characteristics are the precursor to more in-depth evaluations that consider other factors including water depth, exposure to extreme sea conditions, seabed structure and ecological sensitivity, proximity to the national electricity grid as well as competition with other activities.

The wave power energy flux  $\bar{P}$  (in  $kW m^{-1}$ ) available in a certain location is calculated on the basis of scatter diagrams derived from wave measurements or numerical calculations. A scatter diagram shows the average occurrence frequency (in %) of different sea states for one year (or one month) and a given wave direction. A sea state is defined by a combination of Significant Wave Height  $H_s$  and Mean Wave Period  $T_m$  both derived from spectral analysis:  $H_s = 4\sqrt{m_0}$ ;  $T_m = \sqrt{\frac{m_0}{m_2}}$  where  $m_n$  is the  $n^{\text{th}}$  moment of spectral density. Table 1 is the average scatter diagram for all wave directions calculated from the wave buoy observations for the period 14<sup>th</sup> September 2011 to 13<sup>th</sup> September 2012.  $H_s$  values are centred at intervals of 0.5m and  $T_m$  values in intervals of 1s.

**Table 1:** Scatter diagram for wave buoy data from 14/9/2011 to 13/9/2012

significant wave height /m	Mean absolute wave period /s									
	0	1	2	3	4	5	6	7	8	9
0.5	0	0.16	15.21	16.62	1.81	0.16	0	0	0	0
1.0	0	0	0.52	15.41	6.75	0.81	0.05	0	0	0
1.5	0	0	0	3.85	9.72	1.18	0.07	0	0	0
2.0	0	0	0	0.12	6.57	1.95	0.05	0	0	0
2.5	0	0	0	0	2.15	3.12	0.21	0	0	0
3.0	0	0	0	0	0.09	2.86	0.34	0.02	0	0
3.5	0	0	0	0	0	1.05	0.76	0.09	0	0
4.0	0	0	0	0	0	0.09	0.71	0.03	0	0
4.5	0	0	0	0	0	0.01	0.60	0.04	0	0
5.0	0	0	0	0	0	0	0.2	0.26	0	0
5.5	0	0	0	0	0	0	0.07	0.26	0.01	0
6.0	0	0	0	0	0	0	0	0.13	0.01	0
6.5	0	0	0	0	0	0	0	0.07	0.01	0
7.0	0	0	0	0	0	0	0	0.01	0.03	0
7.5	0	0	0	0	0	0	0	0.01	0.01	0
8.0	0	0	0	0	0	0	0	0	0	0

For each state in a scatter diagram the corresponding wave power is calculated by the expression:

$$\bar{P} = \frac{\rho g^2}{64\pi} H_s^2 T_m = 0.490 H_s^2 T_m,$$

where water density is 1.025 Kg m<sup>-3</sup> and g is 9.807 m s<sup>-2</sup>. The total flux is the sum of the contributions of all the waves considered in the period of interest,

and calculated by:  $\bar{P} = 0.490 \sum (H_s^2 T_m) \alpha_{ij}$ ,

where the different combinations (i,j) of position in the scatter diagram for wave period and wave height are weighted by the parameter  $\alpha_{ij}$  expressing the % occurrence for which the different combinations are present. In the case of an average over a full year,

$\bar{P} * 8760$  gives the available wave power per year per metre wavefront in MWh.

Statistics and wave power calculations for data spanning the whole period of buoy deployment are presented in Figure 4 and Tables 2 and 3. Data are also analysed in batches: Autumn (14<sup>th</sup> September 2011–30<sup>th</sup> November 2011), Winter (1<sup>st</sup> December 2011–29<sup>th</sup> February 2012), Spring (1<sup>st</sup> March 2012–31<sup>st</sup> May 2012) and Summer (1<sup>st</sup> June 2012–13<sup>th</sup> September 2012), to identify the seasonal variability. These results compare well with those derived from the tuned SWAN model at the same location and for the same period, except that the model underestimates all the values to some extent.

The highest waves ( $H_s > 5m$ ) occurred in the months November 2011 to April 2012 (refer to Table 2), with an absolute maximum  $H_s$  of 7.46m on 6<sup>th</sup> January 2012 during an almost uninterrupted spell of 22 hours with waves exceeding an  $H_s$  of 5m. During the month of June the significant wave height remained below 2.45m. On the lower end, over the whole period of measurement,  $H_s$  is under 1m for more than 50% of the time (Figure 4a), with an equivalent total of 85 days with waves lower than 0.5m, of which 21 days of calm sea states with  $H_s < 0.25$  m. This reflects on the mean significant wave height which is below 2m even during winter (Table 3).

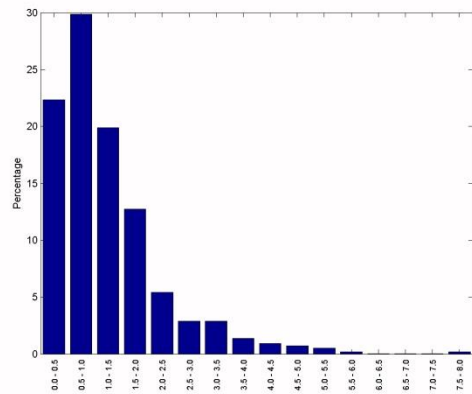


**Figure 4a:** Wave magnitude histogram at the buoy location offshore west of Gozo in the period 14/9/2011 to 13/9/2012

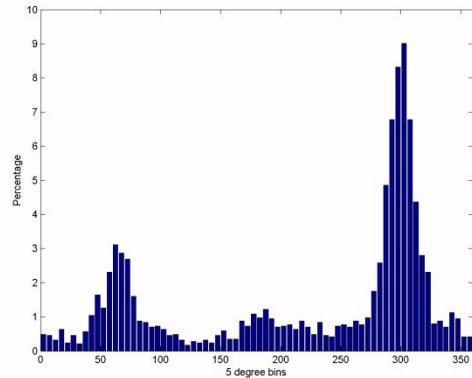


**Figure 4b:** Wave direction histogram at the buoy location offshore west of Gozo in the period 14/9/2011 to 13/9/2012

In parallel to the dominant Mistral wind field to which this location is highly exposed, the sector bounded by West and North West envelopes the most frequent directions from which the waves are incident (Figure 4b). 44% of the waves are coming from these directions with a predominance from N55°W. 15% of the waves come from the North East and are influenced by the proximity of the buoy location close to the western Gozitan headland.

The annual mean wave power transport is found to be  $7.0 \text{ kW m}^{-1}$ , giving an estimated wave power per year of 61.3 GWh for each 1m of wavefront. Table 3 shows that the wave energy in the winter months is more than double the annual mean, but it is below the average for the rest of the year. This is a clear indication of a strong seasonal variability and a wave energy availability that is mainly concentrated in time.

**Table 2:** Maximum Significant Wave Height by month from wave buoy data in the period 14/9/2011 to 13/9/2012

Month	Max Hs /m	Month	Max Hs /m
SEP 2011	3.57	MAR 2012	5.80
OCT 2011	4.08	APR 2012	5.83
NOV 2011	5.92	MAY 2012	4.02
DEC 2011	6.85	JUN 2012	2.45
JAN 2012	7.46	JUL 2012	3.84
FEB 2012	6.75	AUG 2012	3.57

**Table 3:** Key statistics from wave buoy and SWAN data in the period 14/9/2011 to 13/9/2012

	Mean Wave power / $\text{kW m}^{-1}$		Mean Significant Wave Height /m	Maximum Significant Wave Height /m
	Model	Buoy	Buoy	Buoy
Winter	14.0	15.23	1.92	7.46
Spring	4.78	6.03	1.12	5.83
Summer	0.95	1.75	0.70	3.84
Autumn	3.77	3.99	1.53	4.08
Full period	6.17	7.0	1.22	7.46

## 5. WAVE POWER CALCULATIONS FROM SWAN

In the absence of other available wave observations other than those described in section 4, the SWAN model hindcast 3-hourly wave fields, each composed of a total of 89701 grid points around the Maltese Islands, and with an evolution in time spanning five consecutive years (2007 – 2011), provide a unique homogeneous, long-term and high-resolution wave database. The extracted data consist of: significant wave height, mean wave direction, and mean and peak period. Model data time series were extracted, post-processed, and statistical diagnostics describing the wave temporal characteristics derived at each sea grid point. In particular, these time series were used to perform a wave energy resource assessment as described in the previous section. Merging of the results across all the model points was subsequently performed to bring out the spatial variability at the model grid resolution in terms of combined statistics, and by

means of 2D maps of the relevant parameters. The model data are able to quantify the refraction-diffraction and energy dissipation due to bottom friction and thus achieve a high degree of knowledge of the wave climate in the domain. The analysis was made on the full 5-year period as well as on individual years to check for interannual variability.

### 5.1 Model wave height analysis

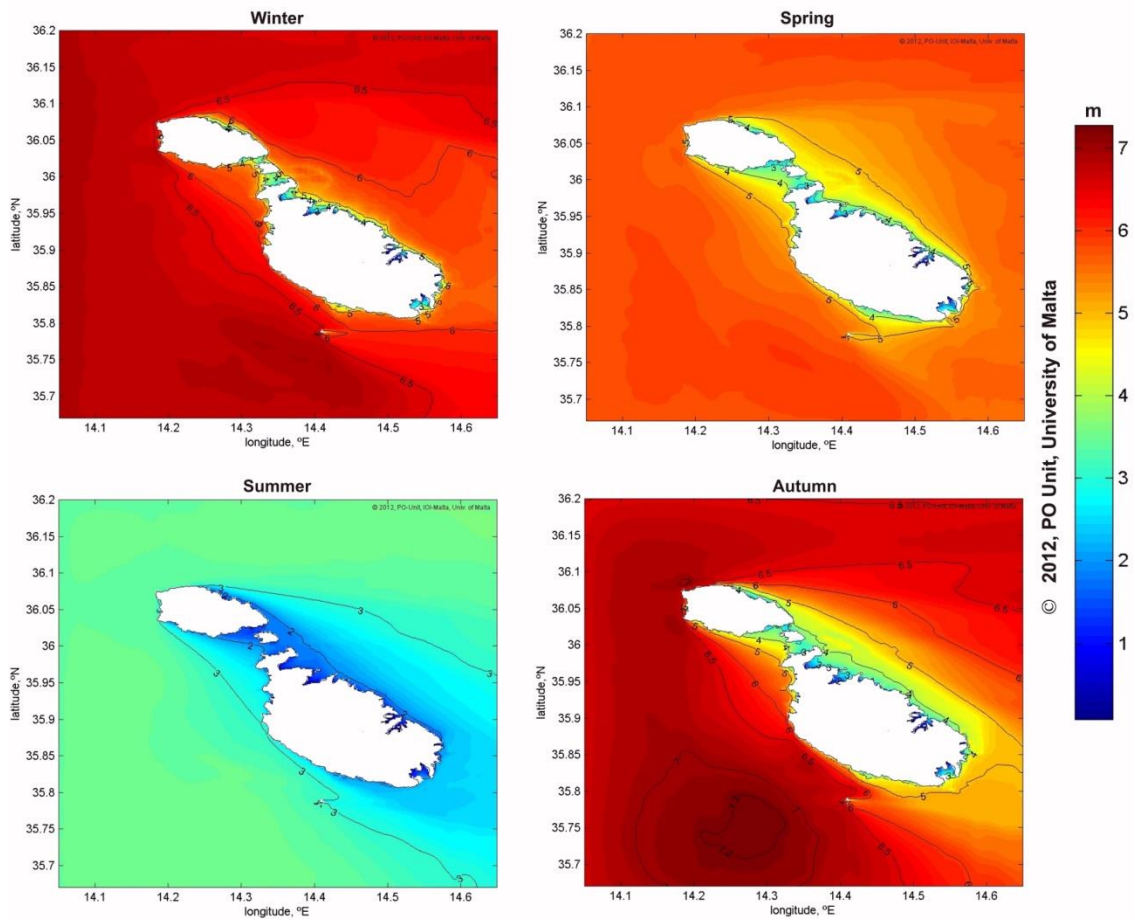
At each SWAN model grid point the data time series of significant wave height was used to calculate: (i) the overall mean for the whole 5-year period, (ii) the seasonal means over the 5-years, and (iii) the annual means for each separate year. Grid point values were integrated into 2D maps for each quantity and to obtain domain-integrated diagnostics. The same procedure was adopted to analyse the occurrence and thresholds of maximum significant wave height on seasonal, annual and interannual timescales.

**Table 4:** Overall, annual and seasonal mean and maximum significant wave height over the SWAN model domain (2007 – 2011)

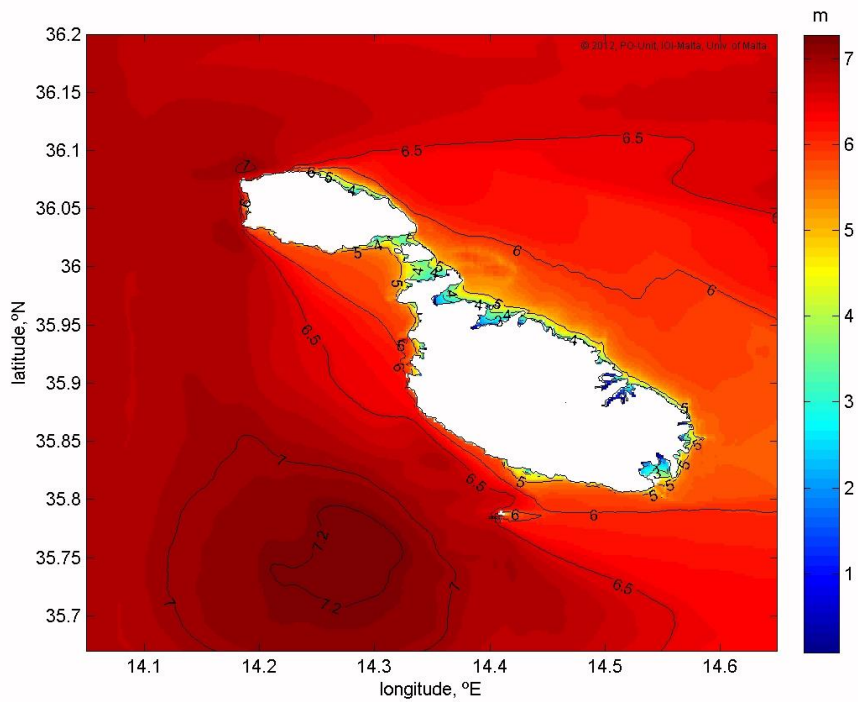
PERIOD	Domain Mean Hs /m	Domain Mean of Max Hs /m	Domain Absolute Max Hs /m
Whole period (2007-2011)	1.22	6.49	7.28
Winter (2007-2011)	1.70	6.40	6.96
Spring (2007-2011)	1.32	5.55	5.95
Summer (2007-2011)	0.72	3.17	3.59
Autumn (2007-2011)	1.18	6.26	7.28
2007	1.18	6.24	7.28
2008	1.03	5.83	6.52
2009	1.16	6.34	6.96
2010	1.19	5.41	5.84
2011	1.05	6.15	6.88

Table 4 attempts to synthesise the large amount of information generated by this exercise. The maps in Figure 5a, provide a synoptic view of the areas with highest waves in the SWAN model domain, on a seasonal basis; the overall maximum  $H_s$  in the domain, calculated for the full five years of model simulation (period: 2007 – 2011), is displayed in Figure 5b.

The interannual variability is not particularly strong with the domain annual mean  $H_s$  just varying in the range 1.05 – 1.19 m across the five years. The highest simulated waves occur in Autumn 2007 with an absolute maximum  $H_s$  of 7.28 m at a location south of Malta; the domain mean of maximal  $H_s$



**Figure 5a:** SWAN model seasonal significant wave height maxima (m) (period: 2007 – 2011)



**Figure 5b:** SWAN model significant wave height maxima (m) (period: 2007 – 2011)



ranges from 5.41 m in 2010 to 6.24 m in 2007. On the contrary the seasonal signal is substantial. As expected the domain mean  $H_s$  is highest (1.7 m) in Winter with values in excess of 1.8 m to the South of Malta and in the North Western approaches to Gozo; it is around 1/3 less in Spring and Autumn, and less than half in Summer. This is indicative of a wave activity that tends to be reinforced mainly in the period from late October to early April, and is milder for the remaining half of the year. In space, the variability in the mean  $H_s$  is not very high (not shown in the figures), especially in the offshore areas where values range to just around 1.4 m, and the shoaling of the milder waves closer to land is rather sharp and restricted to a narrow strip of sea enclosed by a contour very close to the coast.

The high waves are predominantly from the North West. They are much more dependent on the shoaling effects by the bathymetry, and the diffraction and sheltering by the coastline configuration with respect to the direction of wave incidence, as evidenced in Figure 5. The stronger waves occur to the South of Malta (refer Figure 5b) with values of  $H_s$  reaching higher than 7 m. Strong waves reach closer to the shore on the western promontory of Gozo where  $H_s$  maxima of the order of 6.5 m are practically experienced at the coast. These events can be equally strong in the period September to March, and are particularly more frequent in the months between December and February.

## 5.2 Model wave power analysis

This part of the study is intended to map the available wave energy potential in the coastal and offshore areas of the Maltese Islands, and to identify the sites that carry the highest useful wave resource. In this exercise it is critical to also factor the distribution in time of the available wave power. A site may carry high energy content, but only for a limited time; the feasibility for wave energy extraction could be preferable in less intense, but more persistent wave environments.

In the analysis wave power transport estimates were thus first obtained at each model grid point on the basis of the 5 year span of  $H_s$  and  $T_m$  data time series, and using the wave power method of calculation explained in Section 4. The method in Section 5.1 was subsequently repeated to produce a two-dimensional set of time-averaged annual and seasonal wave power estimates spanning the SWAN model domain. Tables 5 and 6 summarise the results in terms of spatial domain means and maxima of these time averaged fields.

**Table 5:** Full period, annual and seasonal mean wave power transport over the model domain (Values in brackets are median values) (SWAN run: 2007 – 2011)

Mean Wave power ( $\text{kW m}^{-1}$ )	WIN	SPR	SUM	AUT	Annual
2007	8.82 (9.68)	5.88 (6.20)	1.43 (1.53)	6.82 (7.22)	5.21 (5.91)
2008	8.50 (8.74)	5.65 (5.96)	1.01 (1.10)	3.97 (4.11)	4.34 (4.91)
2009	14.17 (15.05)	4.90 (5.14)	1.18 (1.26)	4.54 (4.96)	5.57 (6.41)
2010	9.73 (10.50)	4.57 (4.79)	1.82 (2.02)	4.47 (4.76)	4.71 (5.42)
2011	8.47 (9.29)	4.78 (5.21)	1.29 (1.39)	4.13 (4.41)	4.25 (4.78)
Whole Period	9.10 (10.54)	4.73 (5.36)	1.23 (1.44)	4.38 (4.98)	5.25 (5.59)

**Table 6:** Domain Maxima of annual and seasonal mean wave power transports (SWAN run: 2007 – 2011)

PERIOD	Domain Max. of Mean Wave power ( $\text{kW m}^{-1}$ )	PERIOD	Domain Max. of Mean Wave power ( $\text{kW m}^{-1}$ )
Whole period (2007-2011)	6.73	2007	7.35
Winter (2007-2011)	13.15	2008	6.18
Spring (2007-2011)	6.53	2009	8.17
Summer (2007-2011)	1.72	2010	6.84
Autumn (2007-2011)	6.14	2011	5.90

Analysis of the maps and their summary statistics in Table 5 reveal a change in the domain averaged wave energy resource from year to year and seasonally. Years 2009 and 2007 are the most energetic, with a domain mean of over  $5 \text{ kW m}^{-1}$ , the former year carrying some 24% higher wave energy compared to 2011 at the lower end of the range. This interannual variability is dictated by the Winter conditions and is mostly related to the frequency of occurrence of strong events rather than to their intensity. 2009 is most energetic, but not with the highest  $H_s$  which occurred in 2007. This implies that the wave power resource is not necessarily a result of a stronger wave field, but rather depends more on the duration, frequency of occurrence and areal extent of the stronger wave events.

The available wave power has a marked seasonality, typically very energetic during Winter, with domain maxima of the season-averaged wave power reaching up to  $13.15 \text{ kW m}^{-1}$ ; in Spring and Autumn, this factor reaches values just above  $6 \text{ kW}$

$\text{m}^{-1}$  whereas it does not exceed  $1.72 \text{ kW m}^{-1}$  in Summer.

The most energetic waves reside offshore, mainly in the southern area of the domain, below latitude at  $35.7^\circ \text{ N}$ , where the water is deep, and the exposure to local wave energy resources from the far field through the Strait of Sicily is more pronounced (refer to Figure 6b). The available mean wave power reaches  $6.73 \text{ kW m}^{-1}$ . The overall mean value of the wave power transport for the full domain is  $5.25 \text{ kW m}^{-1}$  (Table 5), while the median is  $5.59 \text{ kW m}^{-1}$  so that this wave resource level is available in more than half the spatial extent of the sea in the domain. The  $5 \text{ kW m}^{-1}$  isoline envelopes

the whole Maltese Islands at a distance of a few nautical miles from shore, but reaching very close to the southern coast of Malta, and in particular the North West coast of Gozo, rendering the latter area of sea specially amenable to wave energy exploitation, especially in virtue of the proximity to land. In both cases the accessibility is however not very favourable due to the raised levels of the land with respect to mean sea level. The lower values of wave power occur in shallow areas with depth less than 100 m, and naturally in sheltered areas and embayments.

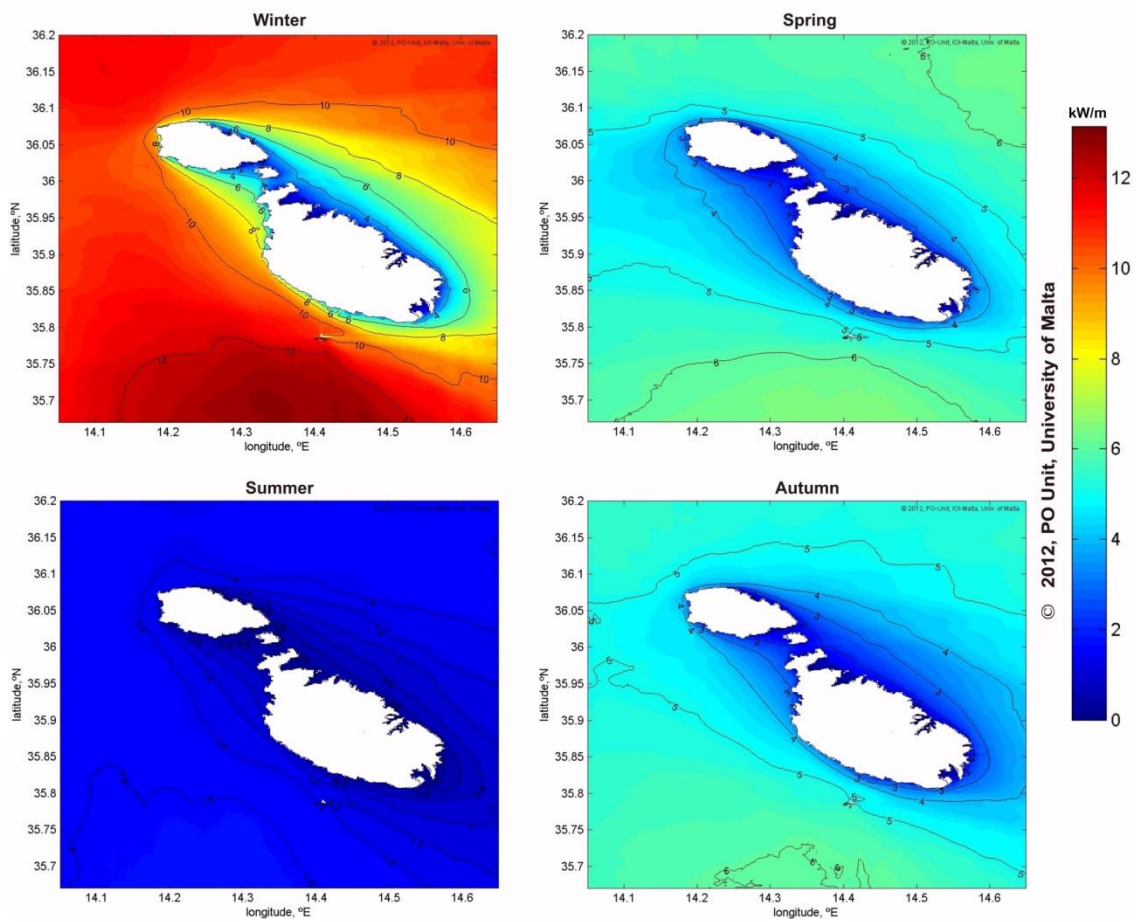


**Figure 6a:** Seasonal mean wave power transport ( $\text{kW m}^{-1}$ ) for SWAN model domain (period: 2007 – 2011)

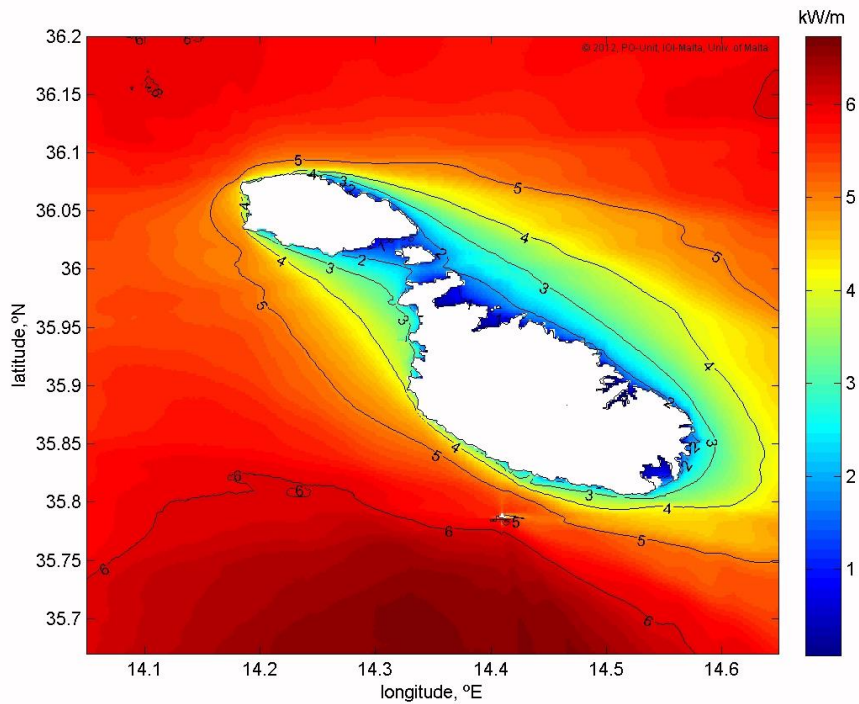


**Figure 6b:** Time averaged wave power transport ( $\text{kW m}^{-1}$ ) for SWAN model domain (2007 – 2011)

## 6. CONCLUSIONS

Assessments on the potential extraction of energy from sea waves require an in-depth analysis of the intrinsic wave properties as well as of their occurrence in time and space. In the absence of sufficient direct measurements, numerical simulations prove to be an indispensable tool to model the wave conditions in a sea area, and to provide exhaustive information for selecting the best candidate sites for energy production. This kind of study was accomplished for the coastal and offshore areas of the Maltese Islands to provide a detailed characterization of the local wave climate and an estimate of the available wave energy potentials. This undertaking availed of SWAN model data over five years (1st January 2007 to 31st December 2011); the model fine tuning and its data validation was made against direct measurements made by a wave buoy deployed west of Gozo.

The results confirm that the wave energy resource in the proximity of the Maltese Islands is about an order of magnitude less than that in the open European western coasts. The relatively deep bathymetry, particularly close to the southern coast of the islands and the northwestern approaches to Gozo, is favourable to high wave intensities closer to shore, and would render infrastructural costs to link to the national electricity grid less expensive. A compromise is however necessary to match the best

wave resourced site with accessibility to the coast which is generally highly elevated with respect to the sea in these areas.

The winter mean wave power transport west of Gozo reaches up to around  $15 \text{ kW m}^{-1}$ , but is only about half this value when it is integrated over a full year. During the summer months the wave power is under  $2 \text{ kW m}^{-1}$ . In fact the variability in wave intensity carries a strong seasonal signal, with most of the energy concentrated in the six months centred about the winter period. The onset of strong wave events can be sporadic and occurring in isolated events that usually last to less than 24 hours, but calm sea states with  $H_s < 0.25 \text{ m}$  are only 1.4% (equivalent to  $\approx 5$  days) in these six months. Without excessive loss in the energy potential, it might be more cost effective to displace the site to just offshore the northernmost tip of Gozo, and closer to Marsalforn where the sub-marine cable from the wave farm would come ashore.

Energy intensive wave fields are also identified at a few kilometres to the South West of Filfla Island where the modelled mean wave power reaches values of  $13 \text{ kW m}^{-1}$  in the winter months; on an annual basis a site close to Filfla can produce close to  $6 \text{ kW m}^{-1}$  worth of energy. This site is however less accessible and at a greater distance from shore, besides the ecological implications linked to the area.

Despite the seasonal variability of the wave power fields, and provided that the right energy extraction technology is employed, wave energy can be considered as a supplementary source of renewable energy. The current feed in tariffs for alternative energy projects, set against the background of the recent slump in photovoltaic technology prices, does not render favourable economic conditions for wave energy production farms at present. As wave energy converters become more efficient and flexible to fit the local wave characteristics, and renewable energy targets become tighter, these conditions may be revised in the near future. In the local scenario, an integrated renewable energy policy would need to consider combining different renewable energy sources, mainly solar in Summer and wind/waves in Winter, to complement for the seasonal dependence of the respective energy resources.

## ACKNOWLEDGMENTS

This project is supported by the National Research and Innovation programme of the Malta Council for Science and Technology, research grant R&I 2010-024 with the participation of Dexawave Energy Malta Ltd.

## REFERENCES

- [1] A. Drago, A study on the sea level variations and the 'Milghuba' phenomenon in the coastal waters of the Maltese Islands, Ph.D Thesis, School of Ocean and Earth Science, University of Southampton (1999).
- [2] Thorpe TW., 2000. The wave energy programme in the UK and the European Wave Energy Network. 4th EWEC, Aalborg, Denmark.
- [3] Waters R, Engstrom J, Isberg J, Leijon M. Wave climate off the Swedish west coast. *Renewable Energy* 2009;34:1600–6.
- [4] V. Vannucchi, Estimation of wave energy potential of the Mediterranean Sea and propagation toward nearshore areas, Inore Symposium, Denmark (2012).
- [5] D. Vicinanza, L. Cappiotti, V. Ferrante and P. Contestabile, Estimation of the wave energy in the Italian offshore. *Journal of Coastal Research*, SI 64 (Proceedings of the 11th International Coastal Symposium), (2011), 613-617. Szczecin, Poland.
- [6] A. Delitala A and A. Speranza A (eds), WERMED—Weatherrouting dans la Méditerranée. Results of the Project. CINFAI, Camerino, (2008).
- [7] A. Orasi, S. Morucci, S. Corsini, A. Drago and C. Nieddu, WERMED Weatherrouting dans la Méditerranée Action 2.2: climatologie des vagues, Technical report in connection with the INTERREG IIIB MEDOCC Program of Communitarian participation, (2006), pp99.
- [8] H. Gunther, K. Hasselmann and P.A.E Janssen, The WAM Model Cycle 4, Edited by Modellberatungsgruppe, Hamburg. (1992), Report No.4
- [9] B. Welander, Principles of Wave Energy, Ship & Offshore (2010), Vol.4 98-100.
- [10] H. Gunther, K. Hasselmann and P.A.E Janssen, Report NO.4, The WAM Model Cycle 4, Edited by *Modellberatungsgruppe, Hamburg* Scientific and Technical Documentation, Delft University of Technology (1992).
- [11] SWAN Scientific and Technical Documentation, Delft University of Technology, (2013). [http://swanmodel.sourceforge.net/online\\_doc/swantech/swantech.html](http://swanmodel.sourceforge.net/online_doc/swantech/swantech.html).
- [12] Datawell, Second generation non-directional wave height measuring buoy, [http://download.datawell.nl/documentation/datawell\\_brochure\\_wr-sg\\_b-33-04.pdf](http://download.datawell.nl/documentation/datawell_brochure_wr-sg_b-33-04.pdf) (2012)